[1.]Ishaque KHAN, [2.]Lalsingh KHALSA, [2.]Vinod VARGHESE

UNSTEADY-STATE HEAT CONDUCTION PROBLEM ON A THICK CIRCULAR PLATE AND ITS ASSOCIATED THERMAL STRESSES

[1-3.]Department of Mathematics, Mahatma Gandhi Science College, Armori, Gadchiroli, INDIA

Abstract: In this paper, an attempt has been made to determine and discuss the quasi-static transient thermal stresses on a thick circular plate subjected to arbitrary heat supply [i.e. $f_1(r)$ on the upper face and $f_2(r)$ on the lower face], while the circular curved surface is thermally insulated. The results are obtained in a series form in terms of Bessel's functions. Some numerical results for the displacement, change in temperature and the stress distributions are shown in figures.
Keywords: temperature distribution, heat conduction, thermal stresses, thick circular plate

INTRODUCTION

The interest on thermal stress problems has grown considerably due to the increased usage of industrial and construction materials. Hence, some concerned been reported the theoretical studies in this regard so far. However, to simplify the analyses, almost all the studies were conducted on the assumption that heat is impacted moreover on the upper face or lower face of the plate, or it is kept insulated, or heat was dissipated with uniform heat transfer coefficients throughout the surfaces. For example, Nowacki [1] has determined the steady-state thermal stresses on a thick circular plate subjected to an axisymmetric temperature distribution on the upper face with zero temperature on the lower face and the circular edge respectively. Sugano [2] analysed the unsteady thermal stress in an infinite thick plate with an axisymmetric heat generation on both of its surfaces using generalised finite Fourier transformation and the Hankel transformation based on Weber-Orr development. Noda et al. [3] investigated the two-dimensional transversely isotropic thick circular plate by applying integral transform technique. Sansalone and Carino [4] used finite element method to study the transient response of thick circular plates and different geometries subjected to point impact of different duration in both the time and the frequency domains. Ootao and Tanigawa [5] considered the theoretical treatment of a two-dimensional coupled thermal stress problem of an orthotropic material using a perturbation technique for temperature and thermoelastic fields. Sherief and Hamza [6] derived two-dimensional problem of a thick plate whose lower and upper surfaces are traction free and subjected to a given axisymmetric temperature distribution considered within the context of the theory of generalized thermoelasticity with one relaxation time using Laplace and Hankel transform techniques. Sharma et al. [7] have developed a mathematical model for predicting the response of a thick thermoelastic axisymmetric solid plate subjected to sudden lateral mechanical and thermal loads. The governing equations of motion and heat conduction have been solved by using Laplace and Fourier transform methods to predict the response of the plate in the physical time domain. The model is also formulated and solved with the help of the finite element method (FEM). Nasser [8, 9] investigated problems due to heat sources in the generalised thermoelastic body. Kulkarni and Deshmukh [10,11] determined quasi-static thermal stresses in a thick annular disc subjected to arbitrary initial temperature on the upper face with the lower face at zero temperature for a steady and unsteady state using the classical method. Recently, Varghese and Khalsa [12,13] have investigated the thermoelastic problem for thick plates with boundary conditions of radiation type, in which sources are generated according to the linear function of the temperatures, which will also satisfy the time-dependent heat conduction equation. Kedar and Deshmukh [14] studied the temperature distribution and thermal stresses on a thick circular plate wherein the arbitrary initial heat flux is provided on the upper surface whereas, the lower and the curved surfaces are kept at zero temperature. The temperature distribution in the plate is determined by solving heat conduction equation using variable separation technique. Very recently, thermoelastic analysis of a thick plate with radiation conditions on its curved surfaces was studied by Kumar at al. [15]. Khan at al. [16] investigated steady state heat conduction problem and its associated stress on a thick annular disc due to arbitrary axisymmetric heat flux based on classical method. Most of the researches carried out by previous authors have not considered any thermoelastic problem for thick plates on which sectional heat in impacted from both sides of the faces. The present investigation deals specifically with the practical problem on a thick circular plate affected by sectional heat supply on its upper face and lower face, whereas, the curved surfaces are kept insulated. In this paper, heat conduction differential equation has been solved at the first instance by using an unconventional classical method. The thermoelastic stresses are determined with the help of suitable Love's function and Goodier's thermoelastic displacement potential function. The results presented here will be more beneficial in engineering problems particularly in thermally induced stress analysis and in determining the state of strain on a thick plate constituting foundations for reactors, pressure vessels, furnaces, etc.

STATEMENT OF THE PROBLEM

Consider a thick circular plate of radius *a* and thickness *h* defined by $0 \le r \le a$, and $-h/2 \le z \le h/2$. Let the plate be subjected to the arbitrary initial temperature over the upper and lower surface (i.e. $z = \pm h/2$). The fixed circular edge $(r = a)$ is thermally insulated as shown in Figure 1.

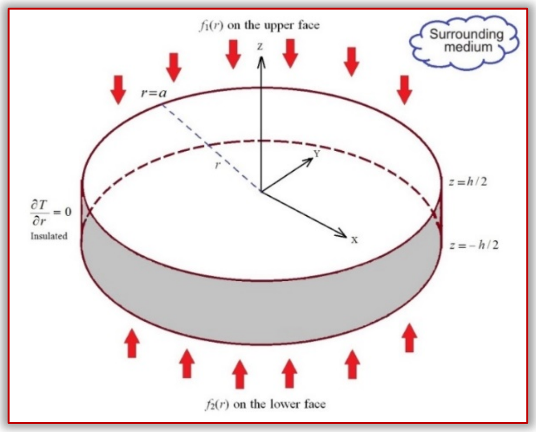

Figure 1. Plate physical configuration

It is assumed that the circular boundary of the thick circular plate is free from traction under considered prescribed conditions. The quasi-static thermal stresses are required to be determined.

— Temperature distribution

The temperature of the plate at time *t* satisfy the heat condition equation

$$\frac{\partial^2 T}{\partial r^2} + \frac{1}{r}\frac{\partial T}{\partial r} + \frac{\partial^2 T}{\partial z^2} = \frac{1}{\kappa}\frac{\partial T}{\partial t} \tag{1}$$

subjected to the initial and boundary conditions

$$T \neq 0 \ \text{at} \ t = 0 \tag{2}$$

$$T = f_1(r) \ \text{at} \ z = h/2 \tag{3}$$

$$T = f_2(r) \ \text{at} \ z = -h/2 \tag{4}$$

$$\frac{\partial T}{\partial r} = 0 \ \text{at} \ r = a \tag{5}$$

in which thermal diffusivity of the material of the plate is denoted as $\kappa = \lambda/\rho C$, λ being the thermal conductivity of the material, ρ is the density and C is the calorific capacity, assumed to be constant.

— Thermal displacements and thermal stress

The Navier's equations in the absence of body forces for axisymmetric two-dimensional thermoelastic problem can be expressed as [17]

$$\left.\begin{aligned} &\nabla^2 u_r - \frac{u_r}{r} + \frac{1}{1-2\upsilon}\frac{\partial e}{\partial r} - \frac{2(1+\upsilon)}{1-2\upsilon}\alpha_t\frac{\partial T}{\partial r} = 0 \\ &\nabla^2 u_z - \frac{1}{1-2\upsilon}\frac{\partial e}{\partial z} - \frac{2(1+\upsilon)}{1-2\upsilon}\alpha_t\frac{\partial T}{\partial z} = 0 \end{aligned}\right\} \tag{6}$$

where u_r and u_z are the displacement components in the radial and axial directions, respectively and the dilatation *e* as

$$e = \frac{\partial u_r}{\partial r} + \frac{u_r}{r} + \frac{\partial u_z}{\partial z} \tag{7}$$

The displacement function in the cylindrical coordinate system is represented by the Goodier's thermoelastic displacement potential ϕ and Love's function *L* as

$$u_r = \frac{\partial \phi}{\partial r} - \frac{\partial^2 L}{\partial r \partial z}, \tag{8}$$

$$u_z = \frac{\partial \phi}{\partial z} + 2(1-\upsilon)\nabla^2 L - \frac{\partial^2 L}{\partial^2 z} \tag{9}$$

in which Goodier's thermoelastic potential ϕ must satisfy the equation

$$\left(\frac{\partial^2}{\partial r^2} + \frac{1}{r}\frac{\partial}{\partial r} + \frac{\partial^2}{\partial z^2}\right)\phi(r,z,t) = K\tau \tag{10}$$

with

$$\phi = 0 \ \text{at} \ t = 0 \tag{11}$$

whereas, the Love's function *L* must satisfy the equation [18]

$$\left(\frac{\partial^2}{\partial r^2} + \frac{1}{r}\frac{\partial}{\partial r} + \frac{\partial^2}{\partial z^2}\right)^2 L(r,z,t) = 0 \tag{12}$$

where $K = (1+\upsilon)\alpha/(1-\upsilon)$ is the resistance coefficient, $\tau = T - T_i$, T_i is the initial temperature condition, τ is the temperature change to be determined from the heat conduction differential equation (1).

The component of the stresses are represented by the use of the potential ϕ and Love's function *L* as

$$\sigma_{rr} = 2G\left\{\frac{\partial^2 \phi}{\partial r^2} - K\tau + \frac{\partial}{\partial z}\left(\upsilon\nabla^2 L - \frac{\partial^2 L}{\partial r^2}\right)\right\}, \tag{13}$$

$$\sigma_{\theta\theta} = 2G\left\{\frac{1}{r}\frac{\partial \phi}{\partial r} - K\tau + \frac{\partial}{\partial z}\left(\upsilon\nabla^2 L - \frac{1}{r}\frac{\partial L}{\partial r}\right)\right\}, \tag{14}$$

$$\sigma_{zz} = 2G\left\{\frac{\partial^2 \phi}{\partial r^2} - K\tau + \frac{\partial}{\partial z}\left((2-\upsilon)\nabla^2 L - \frac{\partial^2 L}{\partial z^2}\right)\right\}, \tag{15}$$

and

$$\sigma_{rz} = 2G\left\{\frac{\partial^2 \phi}{\partial r \partial z} + \frac{\partial}{\partial r}\left((1-\upsilon)\nabla^2 L - \frac{\partial^2 L}{\partial z^2}\right)\right\} \tag{16}$$

in which G is the shear modulus, υ is the Poisson's ratio, and the Laplacian operator presented as

$$\nabla^2 = \frac{\partial^2}{\partial r^2} + \frac{1}{r}\frac{\partial}{\partial r} + \frac{\partial^2}{\partial z^2} \tag{17}$$

The boundary condition on the traction free surface stress functions are

$$\sigma_{zz} = \sigma_{rz} = 0 \quad \text{at} \quad z = -h/2 \tag{18}$$

Equations (1) to (18) constitute the mathematical formulation of the problem.

SOLUTION TO THE PROBLEM

— Solution of temperature change

We assume that the expression for temperature distribution as

$$T(r,z,t) = \cosh(z + h/2)\sum_{n=1}^{\infty} f_n(t) J_0(\alpha_n r) \tag{19}$$

where $f_n(t)$ will be determined from heat conduction equation, $J_1(\alpha_n, a)$ is the Bessel function of the first kind of order one, and $\alpha_1, \alpha_2 ......$ are the roots of the equation $J_1(\alpha_n, a) = 0$ respectively.

Using equation (19) in (1) and integrating, one obtains

$$f_n(t) = A_n \exp[\kappa(1-\alpha_n^2)t] \tag{20}$$

in which the constant A_n can be determined from the nature of temperature prescribed on the lower and upper faces.

Taking into account the boundary conditions (3) and (4), the assumed temperature equation (19), and equation (20), we have

$$f_1(r) + f_2(r) = [\cosh(h)+1]\sum_{n=1}^{\infty} A_n J_0(\alpha_n r)\exp[\kappa(1-\alpha_n^2)t] \tag{21}$$

By using the theory of Bessel's function, we arrive at a constant value as

$$A_n = \frac{2}{a^2(\cosh h + 1)J_0(\alpha_n a)}\int_0^a r[f_1(r)+f_2(r)]J_0(\alpha_n r)dr \tag{22}$$

Using equations (19) and (20), we arrive at the solution of the temperature distribution stated above as

$$T = \cosh(z+h/2)\sum_{n=1}^{\infty} A_n J_0(\alpha_n r)\exp[\kappa(1-\alpha_n^2)t] \tag{23}$$

Now the initial temperature T_i is given by $t = 0$ as

$$T_i = \cosh(z+h/2)\sum_{n=1}^{\infty} A_n J_0(\alpha_n r) \tag{24}$$

Taking into account the equations (23) and (24) in the expression $\tau = T - T_i$, the temperature change is finally represented by

$$\tau = \cosh(z+h/2)\sum_{n=1}^{\infty} A_n J_0(\alpha_n r)\{\exp[\kappa(1-\alpha_n^2)t]-1\} \tag{25}$$

— Solution of the thermal stress problem

Referring to the fundamental equation (1) and its solution (25) for the heat conduction problem, the solution for the displacement function are represented by the Goodier's thermoelastic displacement potential governed by equation (10) represented by

$$\phi = D_n \cosh(z+h/2)\sum_{n=1}^{\infty} A_n J_0(\alpha_n r)\{\exp[\kappa(1-\alpha_n^2)t]-1\} \tag{26}$$

Using equation (26) in equation (10), one attains

$$D_n = K/\alpha_n^2 \tag{27}$$

Substituting equation (27) into equation (26), the displacement potential ϕ is indicated by

$$\phi(r,z,t) = K\cosh(z+h/2)\sum_{n=1}^{\infty} A_n J_0(\alpha_n r)\{\exp[\kappa(1-\alpha_n^2)t]-1\}/\alpha_n^2 \tag{28}$$

Similarly, the solution for Love's function L are assumed so as to satisfy the governed condition of equation (12) as

$$\begin{aligned} L(r,z,t) = \sum_{n=1}^{\infty} A_n J_0(\alpha_n r)\{H_n \cosh[\alpha_n(z+h/2)] \\ + R_n \alpha_n z \sinh[\alpha_n(z+h/2)]\}\{\exp[\kappa(1-\alpha_n^2)t]-1\}/\alpha_n^2 \end{aligned} \tag{29}$$

In this manner, two displacement functions in the cylindrical coordinate system (i.e. ϕ and L) are fully formulated. Now, in order to obtain the displacement components, we substitute the values of thermoelastic displacement potential ϕ and Love's function L in equations (8) and (9) and we get

$$\begin{aligned} u_r = \sum_{n=1}^{\infty} A_n \alpha_n J_1(\alpha_n r)\langle -K\cosh(z+h/2) + \alpha_n\{H_n \sinh[\alpha_n(z+h/2)] \\ + R_n[\alpha_n z\cosh(\alpha_n(z+h/2)) + \sinh(\alpha_n(z+h/2))]\}\rangle \\ \times\{\exp[\kappa(1-\alpha_n^2)t]-1\}/\alpha_n^2, \end{aligned} \tag{30}$$

$$\begin{aligned} u_z = \sum_{n=1}^{\infty} A_n J_0(\alpha_n r)\langle K\sinh(z+h/2) - H_n\alpha_n^2\cosh[\alpha_n(z+h/2)] \\ + R_n\alpha_n^2\{2(1-\upsilon)\cosh[\alpha_n(z+h/2) - \alpha_n z\sinh[\alpha_n(z+h/2)]]\}\rangle \\ \times\{\exp[\kappa(1-\alpha_n^2)t]-1\}/\alpha_n^2 \end{aligned} \tag{31}$$

In this manner, the stress components can be evaluated. By substituting the values of thermoelastic displacement potential ϕ from equation (33) and Love's function L from equation (34) in equations (13), (14), (15) and (16), one acquires

$$\begin{aligned} \sigma_{rr} = 2G\sum_{n=1}^{\infty} \langle K(-\alpha_n)(J_0(\alpha_n r) - J_1(\alpha_n r)/r)\cosh(z+h/2) \\ - K\cosh(z+h/2)\alpha_n^2 A_n J_0(\alpha_n r) + H_n A_n \alpha_n^2(\alpha_n J_0(\alpha_n r) \\ \times J_1(\alpha_n r)/r)\sinh[\alpha_n(z+h/2)] + R_n A_n \alpha_n^2\{\alpha_n 2\nu J_0(\alpha_n r) \\ \times\sinh[\alpha_n(z+h/2)] + (\alpha_n J_0(\alpha_n r) - J_1(\alpha_n r)/r) \\ \times\sinh[\alpha_n(z+h/2)] + \alpha_n z\cosh[\alpha_n(z+h/2)]\}\rangle \\ \times\{\exp[\kappa(1-\alpha_n^2)t]-1\}/\alpha_n^2, \end{aligned} \tag{32}$$

$$\begin{aligned} \sigma_{\theta\theta} = 2G\sum_{n=1}^{\infty} \langle A_n J_0(\alpha_n r)\sinh(z+h/2)/r - K\cosh(z+h/2) \\ \times A_n J_0(\alpha_n r) + H_n A_n \alpha_n^2 J_1(\alpha_n r)/r)\sinh[\alpha_n(z+h/2)] \\ + R_n A_n \alpha_n^2\{\alpha_n 2\nu J_0(\alpha_n r)\sinh[\alpha_n(z+h/2)] + (J_1(\alpha_n r)/r) \\ \times\sinh[\alpha_n(z+h/2)] + \alpha_n z\cosh[\alpha_n(z+h/2)]\}\rangle \\ \times\{\exp[\kappa(1-\alpha_n^2)t]-1\}/\alpha_n^2, \end{aligned} \tag{33}$$

$$\begin{aligned} \sigma_{zz} = 2G\sum_{n=1}^{\infty} \langle KA_n J_0(\alpha_n r)\cosh(z+h/2)/r - K\cosh(z+h/2) \\ \times A_n J_0(\alpha_n r) + H_n A_n \alpha_n^3 J_0(\alpha_n r)\sinh[\alpha_n(z+h/2)] \\ + R_n A_n \alpha_n^3 J_0(\alpha_n r)\{(1-2\nu)\sinh[\alpha_n(z+h/2)] \\ - \alpha_n z\cosh[\alpha_n(z+h/2)]\}\rangle\{\exp[\kappa(1-\alpha_n^2)t]-1\}/\alpha_n^2, \end{aligned} \tag{34}$$

$$\begin{aligned} \sigma_{rz} = 2G\sum_{n=1}^{\infty} \langle KA_n(-\alpha_n)J_1(\alpha_n r)\sinh(z+h/2) \\ + H_n A_n \alpha_n^3 J_1(\alpha_n r)\cosh[\alpha_n(z+h/2)] \\ + R_n A_n \alpha_n^3 J_1(\alpha_n r)\{2\upsilon\cosh[\alpha_n(z+h/2)] \\ + \alpha_n z\sinh[\alpha_n(z+h/2)]\}\rangle\{\exp[\kappa(1-\alpha_n^2)t]-1\}/\alpha_n^2 \end{aligned} \tag{35}$$

— Determination of unknown arbitrary function

In order to satisfy the condition (18) solving the equation (34) and (35) for H_n and R_n we arrive at

$$H_n = 4\upsilon K/\alpha_n^2 h, \; R_n = -2K/\alpha_n^2 h \tag{36}$$

Using these values of equation (36) in equations (30)-(35), the expression for displacement and stresses are obtained. The equations of stresses are rather lengthy. Consequently, the same have been omitted here for the sake of brevity, but have been considered during graphical discussion using MATHEMATICA software.

— Special case

Assume that point impulsive heat source impacts the thick plate as

$$f_1(r) = Q_1\,\delta(r-a),\ f_2(r) = Q_2\,\delta(r-a) \tag{37}$$

in which Q_0 is constant heat flux and $\delta(r-b)$ is the Dirac delta function.

Using (37), equation (22) yields

$$A_n = \frac{2(Q_1+Q_2)}{a(\cosh h+1)J_0(\alpha_n a))} \tag{38}$$

For the sake of simplicity, we will set $A = 2(Q_1+Q_2)/ah$, $B = 2K(Q_1+Q_2)/ah$ and $C = 4KG(Q_1+Q_2)/ah$ in expressions (30)-(35) during the graphical presentation.

NUMERICAL RESULTS, DISCUSSION AND REMARKS

Numerical calculations have been carried out for Aluminum metal plate with physical parameters as $a = 1$ cm, $b = 0.5$ cm, $h = 0.25$ cm, wherein, mechanical material properties are considered as Modulus of Elasticity $E = 6.9\times10^6$ N/cm^2, Shear modulus $G = 2.7\times10^6$ N/cm^2, Poisson's ratio $\upsilon = 0.281$, Thermal expansion coefficient, $\alpha = 25.5\times10^6$ cm/cm-^{0}C, Thermal diffusivity $\kappa = 0.86$ cm^2/sec, Thermal conductivity $\lambda = 0.48$ cal sec^{-1}/cm ^{0}C with $\alpha_n =$ 3.8317, 7.0156, 10.1735, 13.3237, 16.4701, 19.6159, 22.7601, 25.9037, 29.0468, 32.1823 are the positive & real roots of the transcendental equation $J_1(\alpha_n, a) = 0$. In order to examine the influence of heating on the plate, numerical calculation for all variables was performed. Numerical calculations are depicted in the following figures with the help of MATHEMATICA software. Figures 2–4 illustrate the numerical results of temperature distribution, displacements, and stresses of thick circular plate impacted by two sources of sectional heat supply on opposite faces.

Figure 2(a) indicates the temperature distribution along the *r*-direction of the thick plate. The maximum value of temperature magnitude occurs at the outer edge due to additional heat supply. The distribution of the temperature gradient at each instance decreases towards inner edge along the radial direction but is again restricted to finite value due to another sectional heat supply.

As expected, in Figure 2(b), with an increase of time in small values along the *z*-direction, the temperature increases due to thermal deformation occurring with additional sectional heat.

Figure 2(c) illustrates the temperature profile along the time line for different values of *r*. At the center of the core, temperature fluctuation is high compared to the inner and outer edge. This may be due to the accumulation of more heat energy and hence thermal expansion increases giving high tensile force which later stabilises by converging at a particular point.

At first glance, as shown in Figure 2(d), graph follows an exponential curve (increasing form) where temperature grows rapidly at the initial stage, then levels out to some limiting value along *t*-direction for different values of *z*.

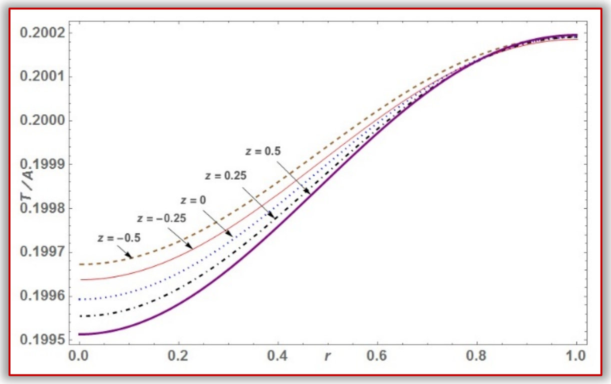

Figure 2(a). Temperature distribution along r for different values of z

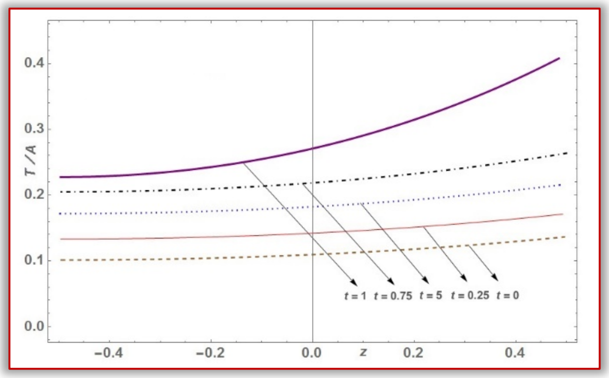

Figure 2(b). Temperature distribution along z for different values of t

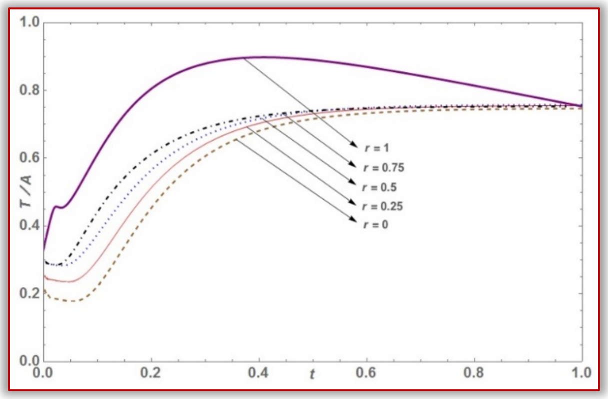

Figure 2(c). Temperature distribution along t for different values of r

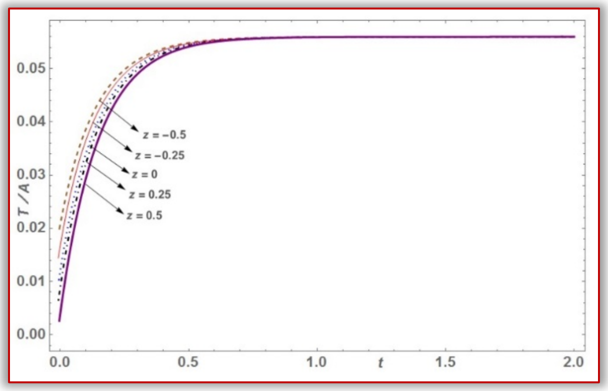

Figure 2(d). Temperature distribution along t for different values of z

Figures 3(a) and 3(b) describe the radial and axial displacement profile along *r*- and *z*-directions. Figure 3(a) indicates that u_r curves were in increasing trend, wherein the curves for u_z are decreasingly stiffer. Thus both displacement profiles have an opposite characteristic, but combined effect nullifies their magnitude variation effects. In Figure 3(b), u_r curves are mostly following a bell-shaped curve (i.e. zero at both the extreme ends and having maximum magnitude at the center) and u_z curves are sinusoidal in nature along the radial direction.

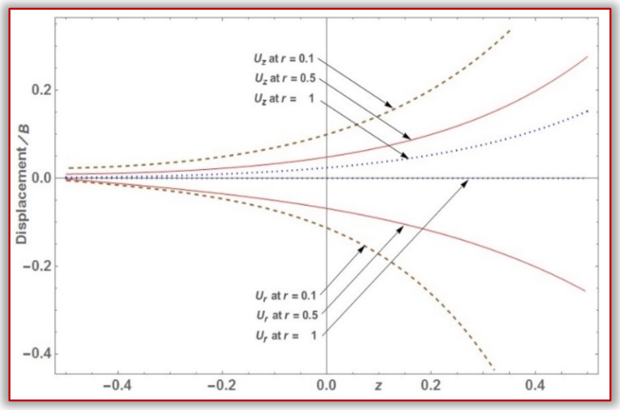

Figure 3(a). Displacement profile along z
for different values of r

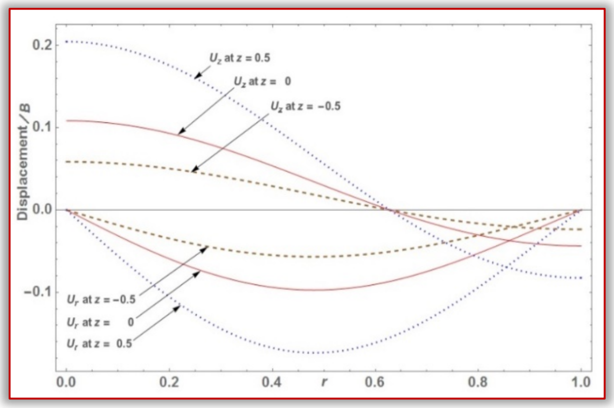

Figure 3(b). Displacement profile along r
for different values of z

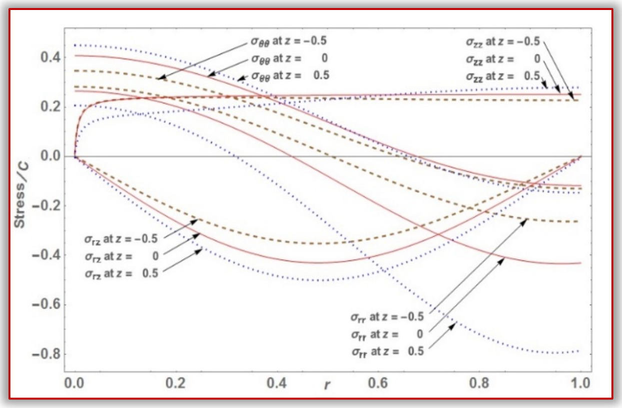

Figure 4(a). Stresses profile along r-direction
for different values of z

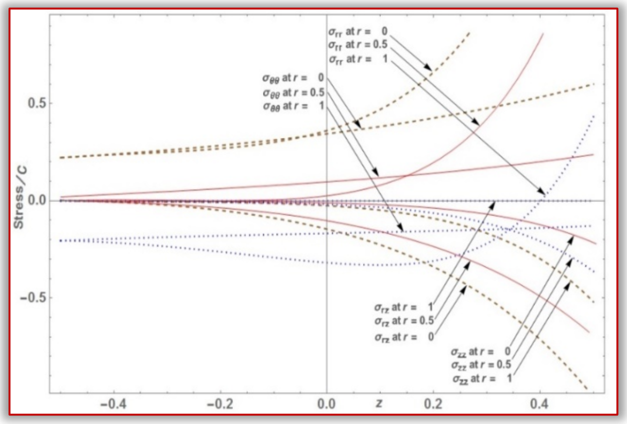

Figure 4(b). Stresses profile along z-direction
for different values of r

Figures 4(a) and 4(b) depicts the combined graphs of radial, circumferential, axial and shear thermal stresses to view at a single glance.

In Figure 4(a), the radial and tangential stress curves are following a decreasing trend, that is, initially stresses are at a higher absolute value which gradually drops along the radial direction. It could be due to compressive forces existing within the concentric region. The axial stress rapidly takes increasing exponential nature which later on stabilises itself along the radial direction at different *z*. The variation of shear stresses response is maximum at the end points through-the-radial direction, while the thermal stress response is minimum on the interior so that the outer edge tends to expand more under tensile stress than the inner part being under tensile stress. In Figure 4(b), almost all stresses gradually increase along *z*-direction for values of *r*.

The σ_{rr} and $\sigma_{\theta\theta}$ curves are similar in nature. It was observed that initially stresses are minimum, but as it approaches towards the outer edge, it gradually increases due to the sources of heat. Stresses σ_{rz} and σ_{zz} curves depict that it initially attains zero at the inner boundary, but increases towards the outer edge along the *z*-axis for different values of *r*. This could owe due to thermal expansion due to external heat supply.

CONCLUDING REMARKS

In this problem, a thick circular plate has been considered for theoretical investigation for determining the expressions for temperature change, displacements and stress functions. As a particular case, the mathematical model is composed of two different sectional heat sources that were impacted on the lower and upper faces. The numerical calculations were performed and plotted graphically.

From the graphs, it is evident that there is a significant impact on the deformation of various components of stresses, displacement, conductive temperature and temperature change in the thick circular plate when impacted with two separate heat supplies. The following results were obtained while carrying out the research work:

- The advantage of this method is its generality and its mathematical power to handle different types of mechanical and thermal boundary conditions.
- Comparing the corresponding results by noting the asymptotic behaviour $\cosh(z+h/2)/\cosh(\alpha_n h) \approx \exp[-\alpha_n(-z+h/2)]$, it is observed that the expressions for stress functions are more rapidly convergent.
- The results obtained here are useful in engineering problems, particularly, in determining the state of strain on a thick circular plate. Any particular case of special interest can be derived by assigning appropriate values to parameters and functions involved in the general solution given with the help of equations (32)-(35).

References

[1] W. Nowacki, The state of stresses in a thick circular disk due to temperature field, Bull. Acad. Polon. Sci., Ser. Sci. Techn., 5, 227, 1957.
[2] Y. Sugano, Transient thermal stresses in a transversely isotropic thick plate with a circular hole due to axisymmetric heat generations on the upper and lower surfaces, Nippon Kikai Gakkai Ronbunshu, 47(419), 730-739, 1981.
[3] N. Noda, Y. Takeuti, K. Uemura, Transient thermal stress problem in a transversely isotropic thick plate with a stationary heat supply on its surfaces, Transactions of the Japan Society of Mechanical Engineers Series A, 48(436), 1536-1543, 1982.
[4] M. Sansalone, N.J. Carino, Transient impact response of thick circular plates, Journal of Research of the National Bureau of Standards, 92(6), 355-367, 1987.
[5] Y. Ootao, Y. Tanigawa, Two-dimensional coupled thermal stress analysis of an orthotropic thick plate due to symmetrical heating, Transactions of the Japan Society of Mechanical Engineers Series A, 55 (511), 530-537, 1989.
[6] H.H. Sherief, F.A. Hamza, Generalized thermoelastic problem of a thick plate under axisymmetric temperature distribution. Journal of Thermal stresses, 17(3), 435-452 1994.
[7] J.N. Sharma, P.K. Sharma, R.L. Sharma, Behavior of thermoelastic thick plate under lateral loads, Journal of thermal stresses, 27, pp 171-191, 2004.
[8] M.E. Nasser, Two dimensional problems with heat sources in generalized thermoelasticity, J. Therm. Stresses, 27, 227-239, 2004.
[9] M.E. Nasser, Two dimensional problems for a thick plate with heat sources in generalized thermoelasticity, J. Therm. Stresses, 28: 1227-1241, 2005.
[10] V.S. Kulkarni, K.C. Deshmukh, Quasi-Static Thermal Stresses in a thick circular plate, Applied Mathematical Modeling, Elsevier Publication, 31(8), 1479-1488, 2007.
[11] V.S. Kulkarni, K.C. Deshmukh, Quasi-static thermal stresses in steady state thick circular plate, Journal of Brazilian Society of Mechanical Sciences and Engineering, XXX, (2) 175, 2008.
[12] V. Varghese, V., L. Khalsa, Two-Dimensional transient problem for a thick disc with internal heat source, FME Transactions, Vol. 38, 173-180, 2010.
[13] V. Varghese, L. Khalsa, Transient thermoelastic problem for a thick annular disc with radiation, International Journal of Applied Mathematics and Mechanics, 7 (7), 57-73, 2011.
[14] G.D. Kedar, K.C. Deshmukh, Estimation of temperature distribution and thermal stresses in a thick circular plate, African Journal of Mathematics and Computer Science Research, 4(13), 389-395, 2011.
[15] R. Kumar, N.K. Lamba, V. Varghese, Analysis of thermoelastic disc with radiation conditions on the curved surfaces, Materials Physics and Mechanics, 16, 175-186, 2013.
[16] I.A. Khan, L. Khalsa, V. Varghese, A steady state heat conduction problem in a thick annular disc due to arbitrary axisymmetric heat flux, Nonlinear Analysis and Differential Equations, 4(3), 121-131, 2016
[17] N. Noda, R.B. Hetnarski, Y. Tanigawa, Thermal stresses 2nd Ed., pp 259-261, Taylor and Francis New York, 2003.
[18] A.E.H. Love, A treatise on the mathematical theory of elasticity, 4th Ed, Dover Publications Inc., New York N.Y., 1944.

ISSN: 2067-3809